## Hybrid Biomimetic Materials:

In different studies I encompass aspects of the structured interfaces of hybrid materials. Hybrid materials consist of at least two different classes of materials. Relevant examples are organic-inorganic hybrid materials, such as most biominerals; oriented inorganic particles nucleated on organic substrate films and the capability to control their precise orientation. Control of the mineral phase is another central issue of this field, with the recent interest in amorphous materials and biominerals. The interface between periodic synthetic and biological structures is an organic-biological hybrid material.

***Oriented nucleation of inorganic crystallites***

(Collaboration with Y. Golan)

The capability of organisms to closely control the deposition process of their mineral parts is well documented and is a source for appealing natural examples such as the nacre (mother of pearl). Nacre often serves as a "model-material" for biominerals due to its simple architecture.[1] In nacre, uniform ~0.5μm thick aragonite single crystal platelets are regularly arranged in layers, separated by organic matrix. {figure 1} The individual platelets are aligned with their crystallographic *c* axis normal to the organic matrix sheets and their *a* and *b* axes in the matrix plane. It was suggested that highly acidic proteins, located at the center of each platelet are implicated in the nucleation of the crystals.[2] [3] We attempt to mimic this effect *in-vitro* by minimizing the essential "ingredients" required for nucleation in nacre into (i) **semi-rigid substrate** (ii) **highly acidic surface**. These two requirements are manifested in artificially produced polydiacetylene (PDA) Langmuir films. PDA Langmuir films were demonstrated as very effective templates for crystal nucleation for calcite {figure 2} [4],[5],[6] and lead sulfide, cadmium sulfide, zinc sulfides [7],[8] and silver sulfide [9].

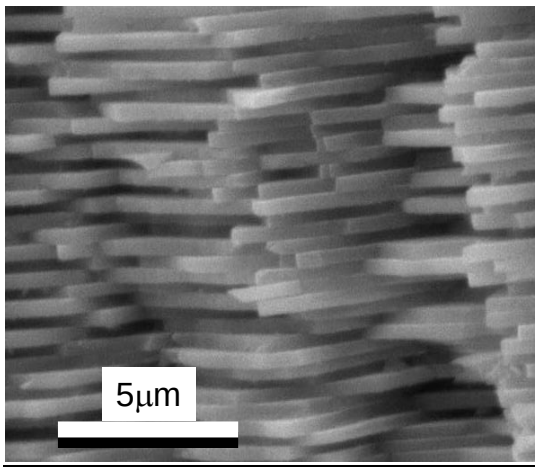


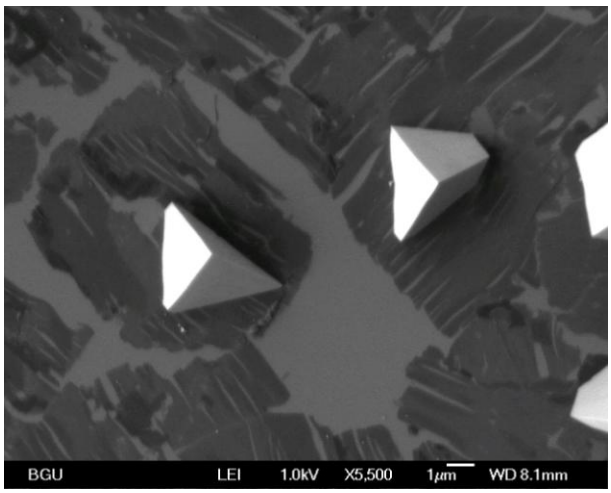


Figure 1: Cross section in nacre from abalone. Note the regular aragonite tablets.

Figure 2: calcite crystals nucleated on PDA on (012) plane. Note that the crystals are aligned with respect to the polymer direction.

***What makes PDA an effective "universal" template for directed nucleation?***

According to our present interpretation, the mechanism is substantially different from epitaxial crystal nucleation as known for inorganic crystals with commensurate structures. At the organic-inorganic interface, due to the pliant nature of the organic substrate, some in-plane structural adaptation can take place. Regular, molecularly dense array of acidic carboxylates groups, presented at the interface, attract cations to the surface and induce local high concentration that may exceed saturation and lead to crystal precipitation. The large 2-D PDA crystals, combined with some structural adjustment to the incipient crystal nucleating plane are likely the principal reasons for the phenomena.
PDA is a polyconjugated polymer that attracts considerable interest due to its two chromatic phases, the transient "blue" phase and the stable "red" phase. PDA sensitivity to various "environmental triggers, makes it a possible substrate for "chromatic biosensors".
In order to gain deeper insight into the details of the organic template nucleation, we embarked on a 2-D crystallography study, using grazing incidence x-ray diffraction (GIXD). The results indicate that considerable surface restructuring takes place during polymerization, and the "blue to red" phase transition [10]. {figure 3} A salient finding of this study is that the different pendant chains, the alkyl and alkanoic acid chains, tethered at the opposite sides of the diacetylene moiety and later, the conjugated backbone, adopt different orientations. We show that the alkyl chains in the monomer and blue phases are highly tilted and arced uniformly in the <11> direction {figure 4}. The principle restructuring during the polymerization step take place by "sliding" of rows of molecules in this direction, thus bringing the diacetylene lipids into the precise distance required for topotactic polymerization. The surface restructuring during the "blue-to red" transformation is associated with the straightening of the alkyl chains toward upright position thus forming a denser close-packed structure.

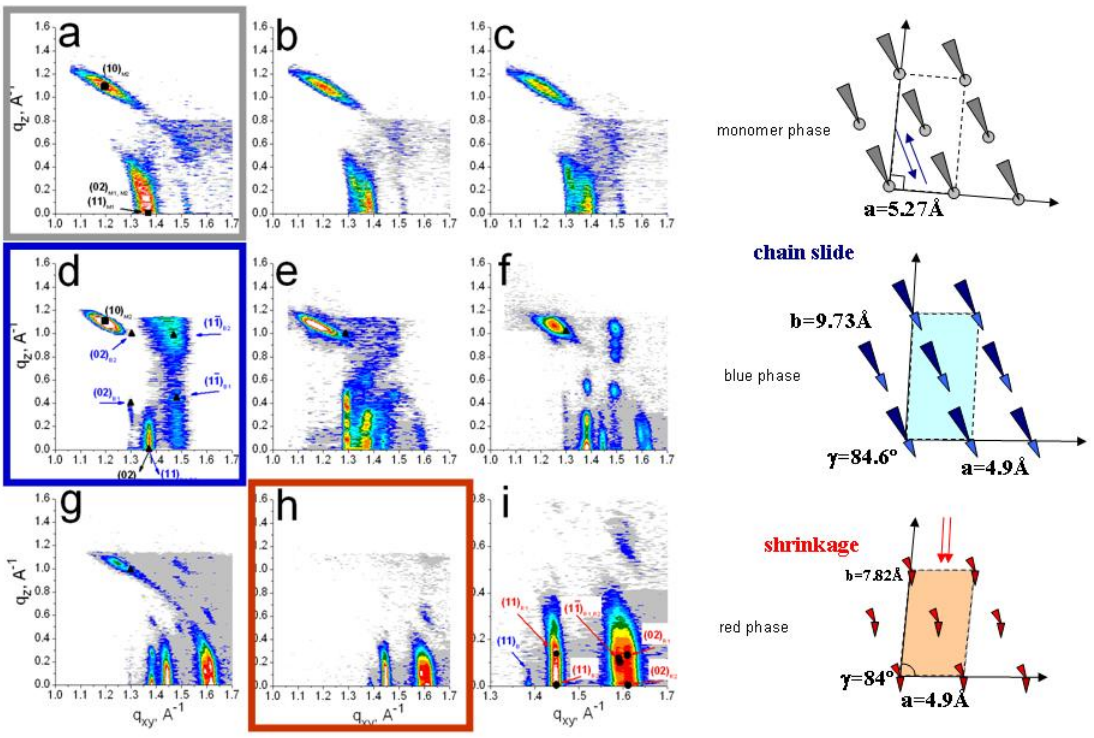


Figure 3: Left: Panels a-h show sequence of 2-D reciprocal maps obtained with GIXD with increasing exposure dose to UV for polymerization and induction of "blue to red" transformation. Panel a-d show gradual polymerization. Panels d-h show discrete blue to red transformation. Right: calculated PDA structures. Panel i is a magnification of h. Monomer phase structure was calculated from a. Blue phase from d and red phase from h.

This in turns cause the distance between the parallel and linear conjugated polymer molecules to shorten, and is manifested in the microscopic strand pattern, typical of PDA. {figure 5}

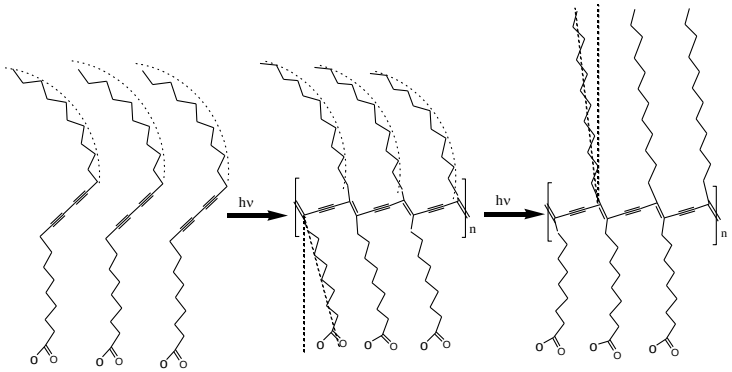


Figure 4: Schematic drawing of PDA in the monomer (left), blue phase (center) and red phase (right), showing the arced alkyl chains in the monomer and blue phases and the nearly upright position in the red phase.

Both in the blue and red phases, the organized carboxylate groups are uniformly, though differently, tilted over the full extent of a single domain. This important stereochemical mechanism acting in the selection of a particular phase is presently systematically studied.

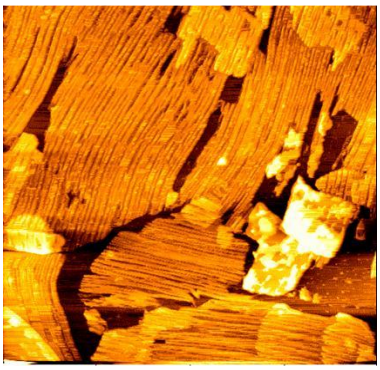

Figure 5 AFM image pf PDA. Note the uniformly aligned extended PDA strands. The conjugated backbone is parallel to the linear morphology. Image size: 4μm.

***Complementary interactions at polydiacetylene interfaces: Biological/organic hybrid material***

PDA ability to change color is sometime recruited for the development of chromatic biosensors. This class of biosensors will change their color or fluorescence response when certain analyte is specifically bound to the surface, by inducing phase transformation from the blue to the red phases. The chromatic/structural response is the outcome of tension or shear forces acting on the conjugated backbone. In most cases the bound analyte bears no structural resemblance to the PDA substrate and is not in registry with it. No wonder though, that such sensors are being developed on empirical grounds, and lack real structural basis.

In order to address this issue, a novel PDA based DNA sensor was designed and studied. Cytosine bearing diacetylenic lipids were synthesized and Langmuir films were formed and polymerized.[11] The defining principle for this sensor and the way it differ other DNA sensors is in its molecular scale geometry. In DNA sensors strands are attached to the surface at one end and the complementary binding takes place perpendicular to the surface (substrate). In our PDA/DNA assembly, the complementary binding takes place on the surface, along the PDA polymer direction. Furthermore, the similarity between the periodic distances in PDA (5Å) and in stretched ssDNA (~6-7Å) allows recognition and base-pair formation at the surface. {figure 6}

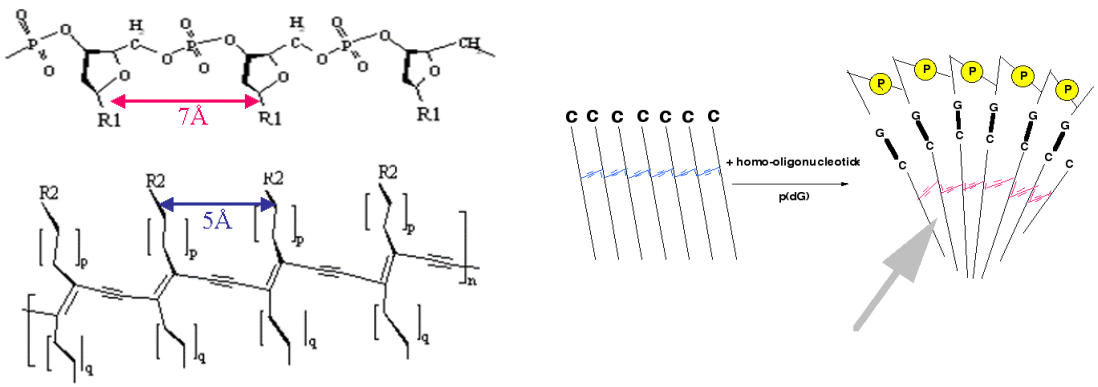


Figure 6. Left: structural formulas of fully extended DNA strand (up) compared with the PDA backbone (bottom). The periodic repeat distances are indicated. R1, R2 denote nucleo-bases. Right: Schematic presentation suggesting the deformation that may take place upon base-pair formation between cytosine derivatized PDA and complementary sequence.

However, upon base-pair formation, they tend to π-stack, just as is the case in dsDNA. In dsDNA, the stacked base pair drives the two strands into the double helix conformation. In our PDA/DNA assembly we expect conformational changes originating from basepair stacking at the interface to cause deformation of the conjugated backbone and result in detectable structural and spectral change. The PDA/DNA system is studied with GIXD. Results so far support our predictions and suggest that indeed the observed arced reflections are associated with deformation of the surface. {figure 7} Raman spectroscopy show that binding of the complementary sequence is manifested in two Raman shifts specific for the "red" phase, while sequences that are not complementary show only the typical "blue" phase Raman shifts. {figure 8}.

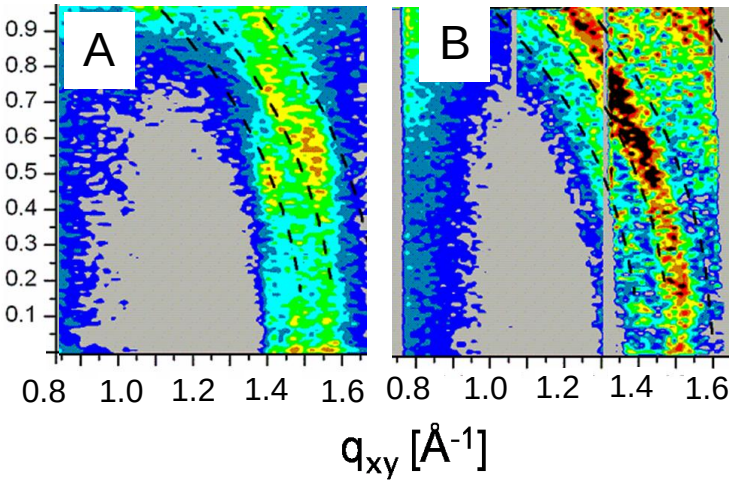


Figure 7: GIXD reciprocal maps showing the 2-D diffraction from PDA derivatized with cytosine monolayer (A), and the same monolayer after incubation with $dG_{12}$ oligonucleotide (B). Note the localized intensity in A compared with the diffraction arcs in B.

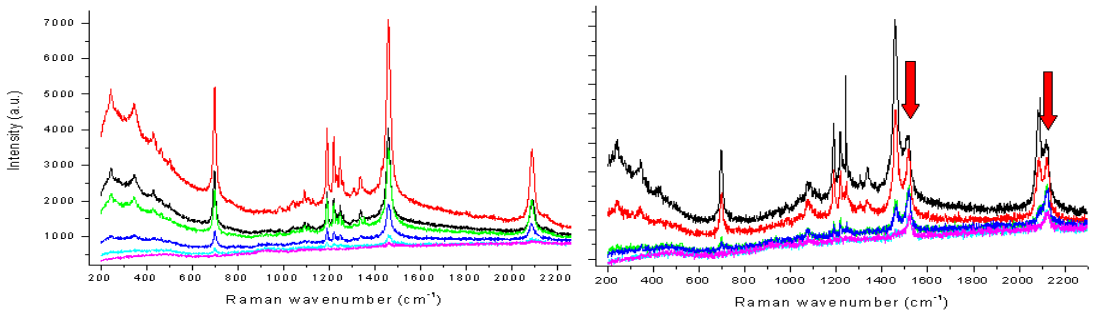


Figure 8: Raman spectra of cytosine derivatized PDA monolayers incubated with non-complementary oligonucleotide ($dC_{12}$), left, and complementary oligonucleotide $dG_{12}$, right. Arrows indicate Raman shifts indicative of the "red" phase PDA. Spectra were taken from top to bottom showing film degradation.

In this study we have demonstrated that by design of the structural properties of the organic interface, we can create an artificial responsive molecular assembly that is based the universal DNA recognition pairs. This principle will be studied in order to control the electronic properties of conjugated polymers, and may be applied in molecular devices as new type of molecular scale DNA sensors.

***In vivo and in-vitro control of amorphous calcium carbonate, ACC***
(Collaboration with A. Sagi)

Amorphous minerals are found in increasing numbers of mineralized tissues. In many cases they transform into the more thermodynamically stable crystalline form within hours or days. This is likely a universal paradigm in biological mineralization that was recently suggested.[12] In some cases, amorphous minerals are stable, and as such fulfill specific roles. For example, the Australian red-claw crayfish, *Cherax quadricarinatus*, the mineralized exoskeleton and special storage organs, the gastroliths, are made entirely of amorphous calcium carbonate (ACC).[13] The gastroliths are very simple spherical mineral constructs made of alternately onion-like sheets of chitin interspersed with ACC and are therefore an ideal model system to study ACC mineralization.
A small number of proteins that are specific to the gastrolith tissue were identified on a SDS gel electrophoresis, of which the most prominent, a 65kD glycoprotein (GAP65) was sequenced. dsRNA carrying a sequence encoding GAP65 was injected to crayfish, "silenced" the expression of the GAP65 and resulted in gastrolith deformation [14].

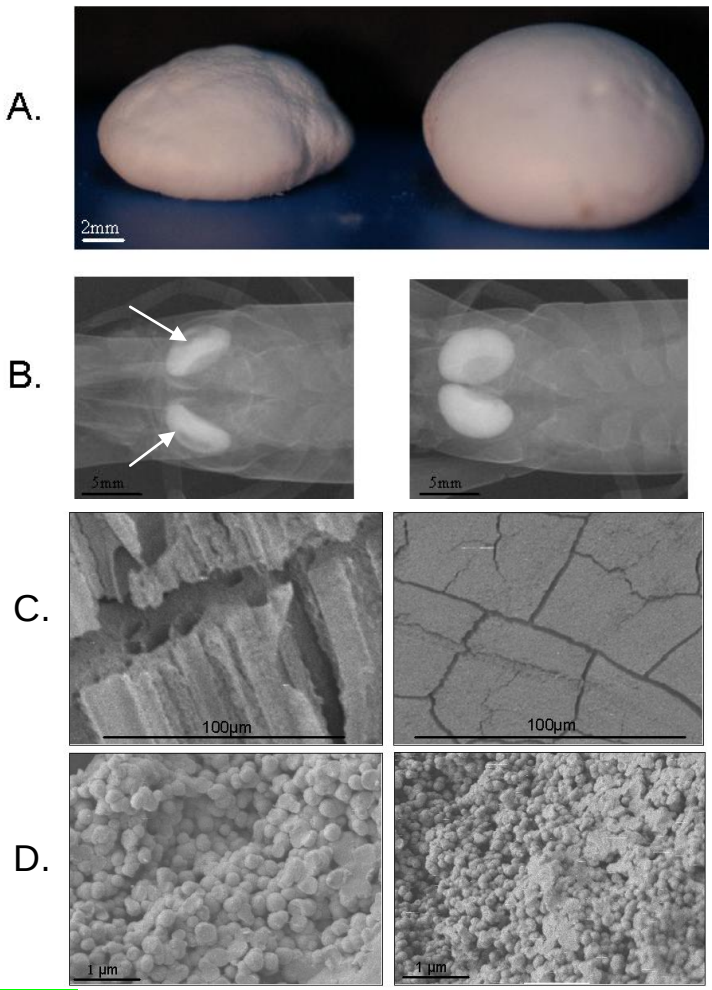


Figure 9 Deformed gastrolith after GAP65 silencing. Left: silenced gastrolith with dsRNA. Right: control ecdysone (molting hormone) only. A: Gastroliths dissected from treated and untreated crayfish. B: X-ray radiographs of the above gastrolith before dissection. Arrows indicate the affected zones where the gastrolith density is most affected. C. Cross-sections of the central part of the gastrolith, demonstrating the mineral and matrix arrangement. (D) ACC mineral spherules. Note the "silenced" gastrolith is composed of larger spherules. (from [14]).

This is the first reported demonstration of "Molecular" intervention in biological mineralization process via "gene silencing"

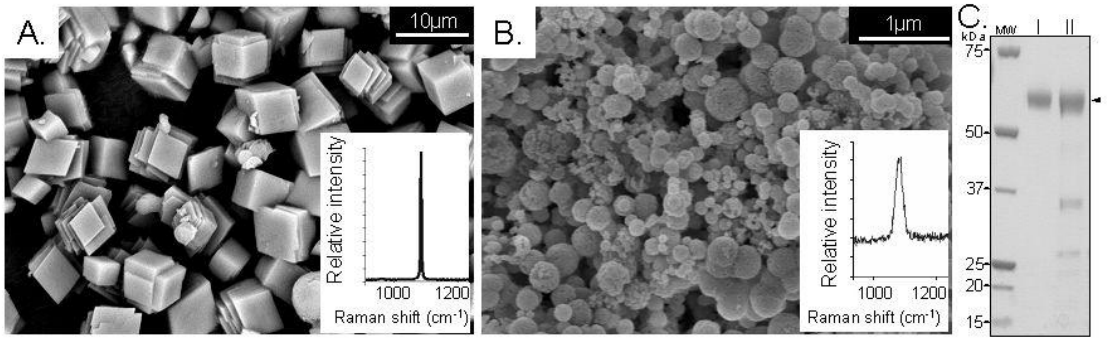


Figure 10: In vitro deposition of calcium carbonate in the absence (A) and in GAP65 presence (B). A shows cleavage rhombohedrons typical of calcite morphology. B depicts spherules typical of ACC. Insets are partial Raman spectra indicating A is calcite, B is ACC. (C) is a SDS gel electrophoresis protein profiles (center, right) of protein extracted from *in-vitro* deposited ACC.

Moreover, the same protein, extracted and added to *in vitro* precipitation experiments induced the formation of stable ACC, compared to calcite in its absence. Hence we conclude that GAP65 plays a crucial role, which is not fully elucidated, in the deposition of ACC and its long-term stabilization. GAP65 sequence contains a chitin binding domain and is also mildly acidic, which hints that it may play a dual role, manifested *in vitro* in the gastrolith deformities and *in-vivo*, in inducing and stabilizing ACC.

***References***


1. Berman, A., *Biomineralization of Calcium Carbonate. The Interplay with Biosubstrates* in *Biomineralization. From Nature to Application*, A. Sigel, H. Sigel, and R.K.O. Sigel, Editors. 2008, John Wiley & Sons, Ltd: Chichester, UK.
2. Levi-Kalisman, Y., et al., *Structure of the Nacreous Organic Matrix of a Bivalve Mollusk Shell Examined in the Hydrated State Using Cryo-TEM.* Journal of Structural Biology, 2001. **135**: p. 8-17.
3. Nudelman, F., et al., *Mollusk shell formation: Mapping the distribution of organic matrix components underlying a single aragonitic tablet in nacre.* Journal of Structural Biology, 2006. **153**(2): p. 176-187.
4. Berman, A., et al., *Total Alignment of Calcite At Acidic Polydiacetylene Films - Cooperativity At the Organic-Inorganic Interface.* Science, 1995. **269**(5223): p. 515-518.
5. Ahn, D.J., A. Berman, and D. Charych, *Probing the dynamics of template-directed calcite crystallization with in situ FTIR.* Journal of Physical Chemistry, 1996. **100**(30): p. 12455-12461.
6. Berman, A. and D. Charych, *Oriented nucleation of inorganic salts on polymeric long chain acid monolayers.* Journal of Crystal Growth, 1999. **199**: p. 796-801.
7. Belman, N., et al., *Transmission electron microscopy of epitaxial PbS nanocrystals on polydiacetylene Langmuir films.* Nanotechnology, 2004. **15**(4): p. S316-S321.
8. Lifshitz, Y., et al., *Template Growth of Nanocrystalline PbS, CdS, and ZnS on a Polydiacetylene Langmuir Film: An In Situ Grazing Incidence X-ray Diffraction Study.* Advanced Functional Materials, 2006. **16**(18): p. 2398-2404.

9. Belman, N., Y. Golan, and A. Berman, *Nanocrystalline Ag2S on polydiacetylene Langmuir films.* Crystal Growth & Design, 2005. **5**(2): p. 439-443.
10. Lifshitz, Y., et al., *Structural Transitions in Polydiacetylene Langmuir Films.* Langmuir, 2008. **(in press)**(XX): p. 000-000.
11. Chen, J. and A. Berman, *Formation of nucleotide base-pairs at the interface of a polydiacetylene cytosine derivatized monolayer.* Nanotechnology, 2004. **15**(4): p. S303-S315.
12. Addadi, L., S. Raz, and S. Weiner, *Taking Advantage of Disorder: Amorphous Calcium Carbonate and Its Roles in Biomineralization.* Adv. Mater., 2003. **15**(12): p. 1-12.
13. Shechter, A., et al., *Reciprocal Changes in Calcification of the Gastrolith and Cuticle During the Molt Cycle of the Red Claw Crayfish Cherax quadricarinatus.* Biol. Bull. (Woods Hole), 2008 **214**: p. 122-134.
14. Shechter, A., et al., *A gastrolith protein serving a dual role in the formation of an amorphous mineral containing extracellular matrix.* Proc. Natl. Acad. Sci. U S A, 2008. **105**(20): p. 7129-7134.